

An Ultra-Sensitive and Stable Electrochemical Sensor with Expanded Working Range via In-situ Assembly of 3-D Structures Based on MXene/GnR Nanohybrids

Sara Mohseni Taromsari^a, HaoTian Harvey Shi^{a,d}, Saeed Habibpour^e, Sophie Kiddell^a, Aiping Yu^e, Chul B. Park^{a,*}, Hani E. Naguib^{a,b,c,*}

a: Department of Mechanical & Industrial Engineering, University of Toronto, Toronto, Ontario, Canada

b: Department of Materials Science & Engineering, University of Toronto, Toronto, Ontario, Canada

c: Institute of Biomedical Engineering, University of Toronto, Toronto, Ontario, Canada

d: Department of Mechanical & Materials Engineering, University pf Western Ontario, London, Ontario, Canada

e: Department of Chemical Engineering, University of Waterloo, Waterloo, Ontario, Canada

*: Corresponding Authors: naguib@mie.utoronto.ca, park@mie.utoronto.ca

S1. Supplementary Figures, Graphs, Tables and Analyses

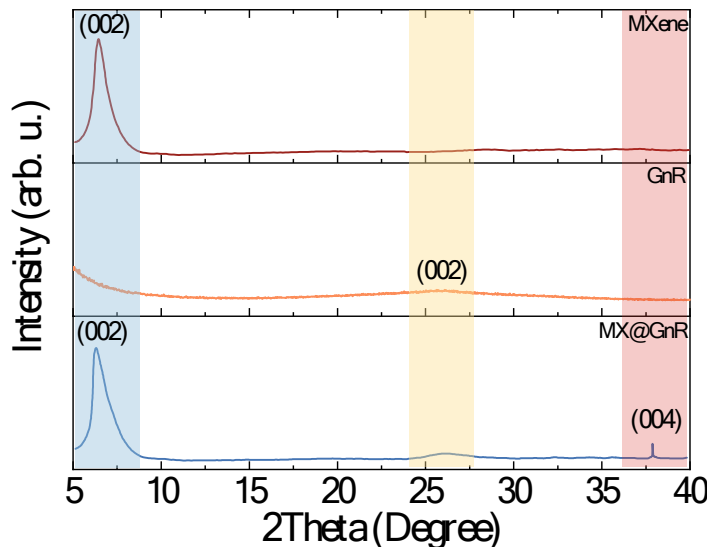


Figure S1. X-ray diffractions spectroscopy of MXene, GnR, MX@GnR.

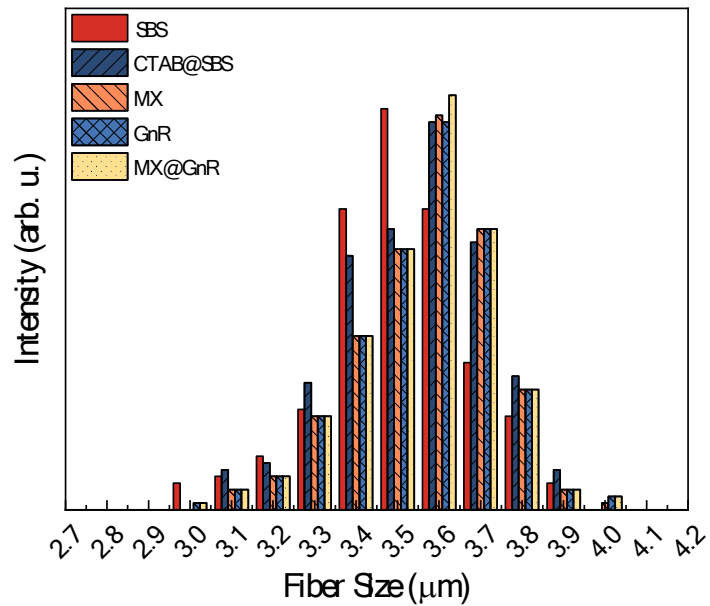


Figure S2. Fiber size distribution histograms taken from 100 fibers in each sample.

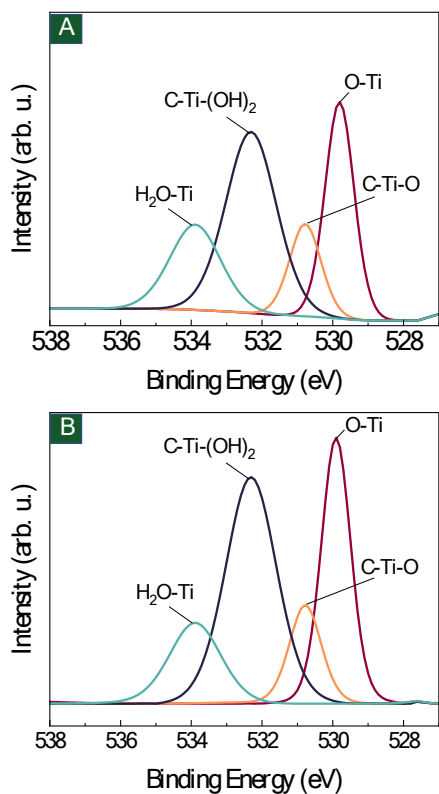


Figure S3- O_{1s} XPS spectra of (A) MX and (B) MX@GnR samples.

Table S1. Electrical Conductivity Values in XYZ Direction*.

Sample Name	Electrical Conductivity at Various Directions		
	X (S/m)	Y (S/m)	Z (S/m)
Neat SBS Membrane	N/A	NA	10 ⁻¹²
MXene Film	95.61	98.63	10 ⁴
GnR Film	24.32	26.22	10 ³
MX	10.96	10.68	10 ⁻¹
GnR	8.12	8.91	1
MX@GnR	12.21	11.75	10
MX@GnR-U	13.52	12.53	10 ⁻⁹
MX@GnR-P	2.63	2.75	10 ⁻¹¹

*: MXene Film and GnR Film samples in the above table, represent neat MXene and GnR powders compacted as films, as identical to MXene and GnR samples in the UPS and UV-vis data. Next, MX and GnR samples represent sensors containing solely MXene or GnR as the conductive coating.

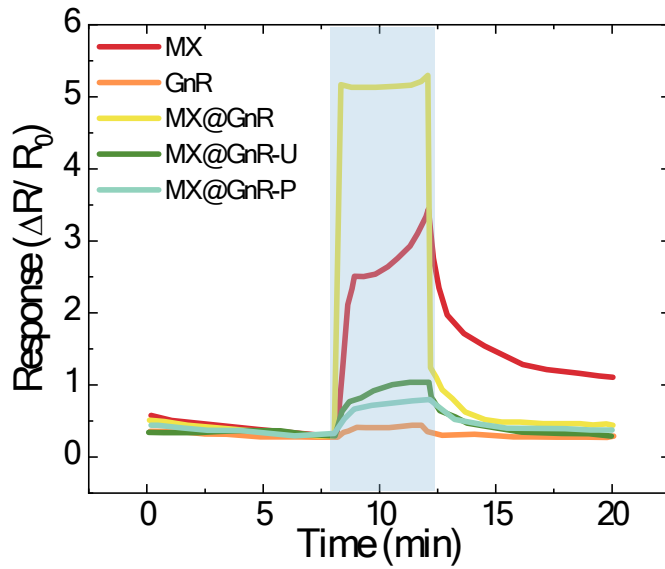
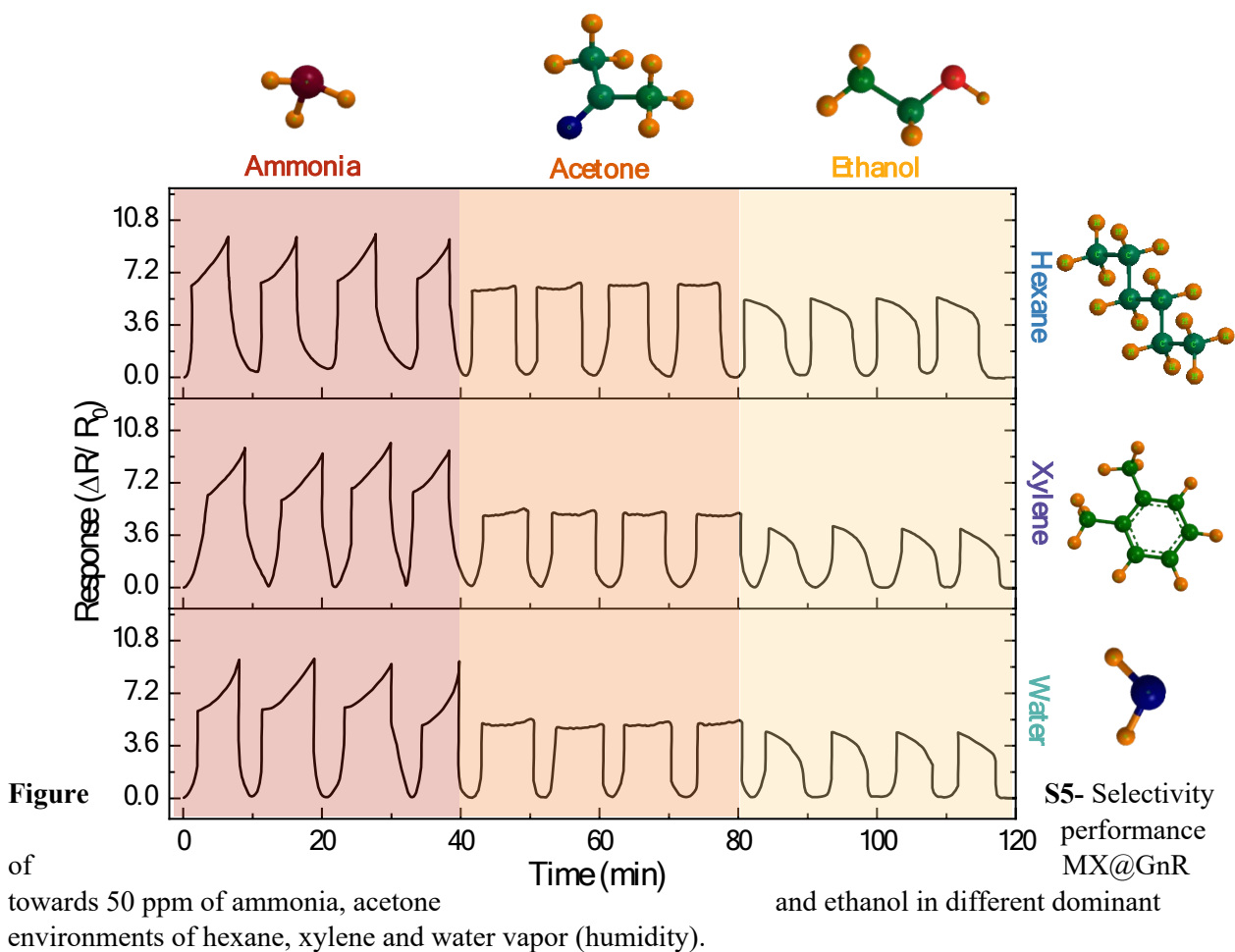
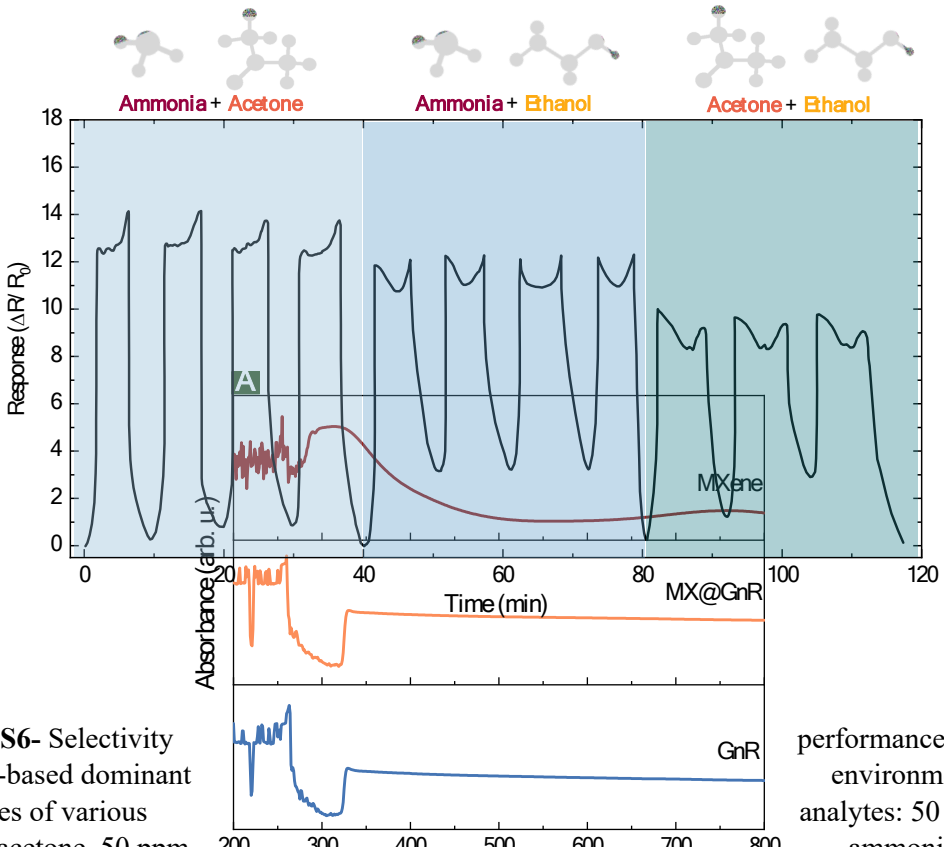


Figure S4. Comparison of gas sensing performance on MX, GnR, MX@GnR, M@GnR-U and Mx@GnR-P sensors.

Table S2- Group-Selectivity Performance of MX@GnR

<i>Group-Selectivity Criteria</i>	<i>Mechanism of Performance</i>	<i>Analytes Performance in the Criteria</i>
<i>Surface polarity</i>	More polarity: more interactions: stronger response [1–3]	Polarity range: acetone>ammonia>ethanol>methanol>NO ₂
<i>H-bonding formation</i>	More H-bonding: formation: more charge transfer: stronger response [4–7]	H-bonding formation capability (measured by DFT studies and VED and BE measurements): ammonia>acetone>ethanol>methanol>NO ₂ >CO ₂
<i>Oxidation/reduction interactions</i>	Due to the formation of electron depleted heterostructures, reducing analytes can produce stronger signals, compared with than oxidizing species [5,8,9]	Reducing analytes: ammonia>acetone>ethanol>methanol (based on electron donating capability and molecular geometry and size) Oxidizing analytes: NO ₂ <CO ₂ (acidic analytes)





performance of MX@GnR environment towards analytes: 50 ppm ammonia ammonia + 50 ppm 50 ppm ethanol.

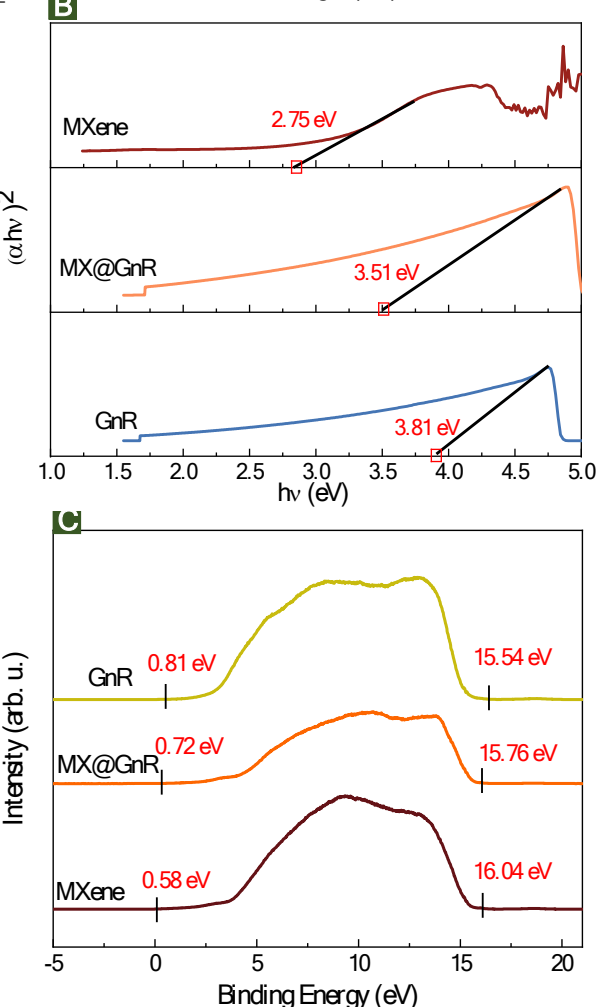


Figure S7. (A) Uv-Vis spectroscopy spectra, (B) Tauc Plots and bandgap values and (C) Ultraviolet photoelectron spectroscopy (UPS) of MXene, GnR and MX@GnR.

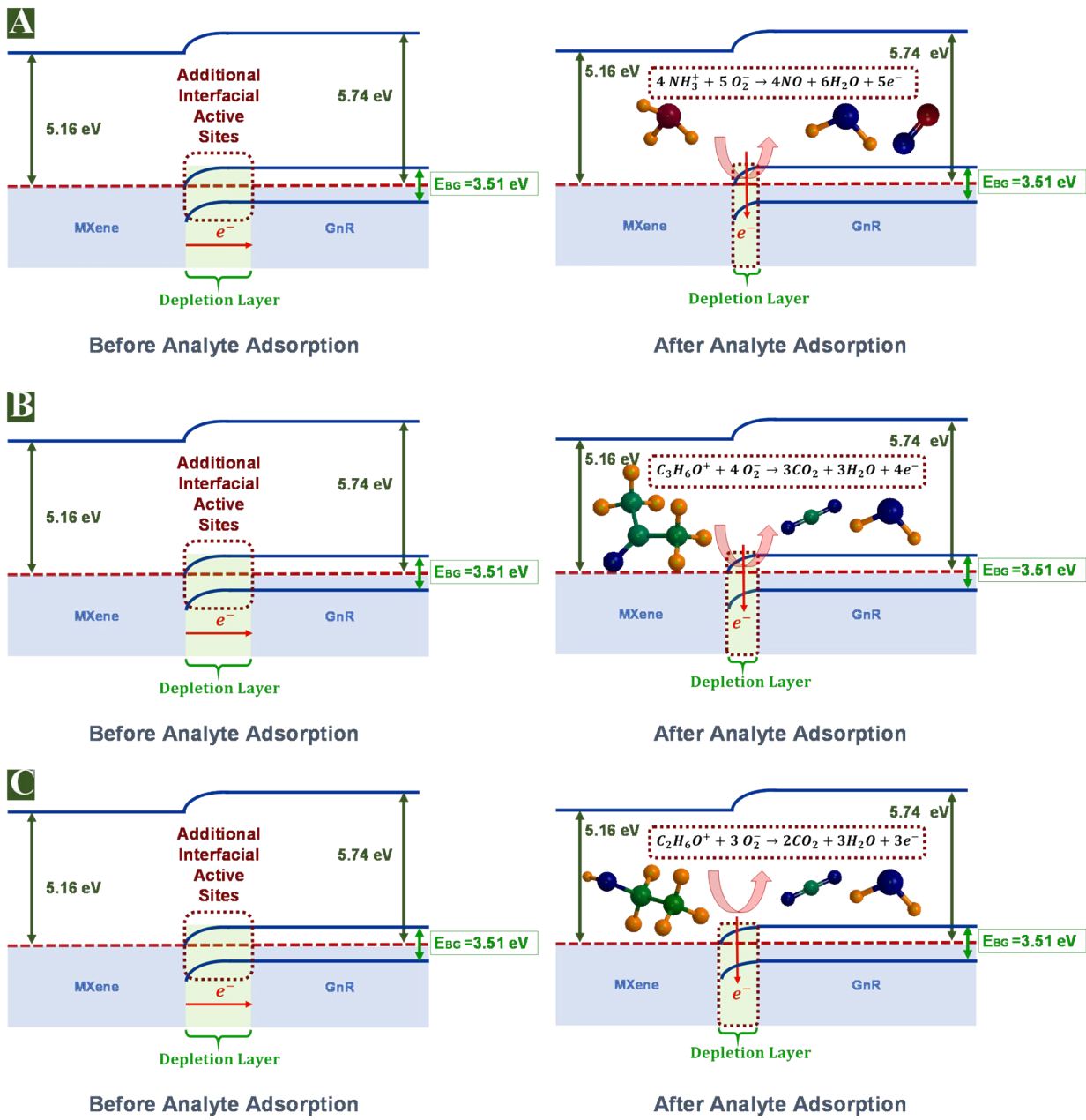


Figure S8. Interfacial heterostructures formed between MXene and GnR and the ox/redox interactions at the depletion layer in the presence of (A) ammonia, (B) acetone, and (C) ethanol.

References

- [1] M. Shekhirev, A. Lipatov, A. Torres, N.S. Vorobeva, A. Harkleroad, A.

- Lashkov, V. Sysoev, A. Sinitskii, Highly Selective Gas Sensors Based on Graphene Nanoribbons Grown by Chemical Vapor Deposition, *ACS Appl. Mater. Interfaces*. 12 (2020) 7392–7402.
<https://doi.org/10.1021/acsami.9b13946>.
- [2] R. Bhardwaj, A. Hazra, MXene-based gas sensors, *J. Mater. Chem. C*. 9 (2021) 15735–15754. <https://doi.org/10.1039/d1tc04085e>.
- [3] K. Deshmukh, T. Kovářík, S.K. Khadheer Pasha, State of the art recent progress in two dimensional MXenes based gas sensors and biosensors: A comprehensive review, *Coord. Chem. Rev.* 424 (2020).
<https://doi.org/10.1016/j.ccr.2020.213514>.
- [4] M.M. Pour, A. Lashkov, A. Radocea, X. Liu, T. Sun, A. Lipatov, R.A. Korlacki, M. Shekhirev, N.R. Aluru, J.W. Lyding, V. Sysoev, A. Sinitskii, nanoribbons with improved electrical conductivity for efficient gas sensing, *Nat. Commun.* (n.d.) 1–9. <https://doi.org/10.1038/s41467-017-00692-4>.
- [5] W.Y. Chen, X. Jiang, S.N. Lai, D. Peroulis, L. Stanciu, Nanohybrids of a MXene and transition metal dichalcogenide for selective detection of volatile organic compounds, *Nat. Commun.* 11 (2020) 1–10.
<https://doi.org/10.1038/s41467-020-15092-4>.
- [6] S.J. Kim, H.J. Koh, C.E. Ren, O. Kwon, K. Maleski, S.Y. Cho, B. Anasori, C.K. Kim, Y.K. Choi, J. Kim, Y. Gogotsi, H.T. Jung, Metallic Ti₃C₂Tx MXene Gas Sensors with Ultrahigh Signal-to-Noise Ratio, *ACS Nano*. 12 (2018) 986–993. <https://doi.org/10.1021/acsnano.7b07460>.
- [7] S.H. Lee, W. Eom, H. Shin, R.B. Ambade, J.H. Bang, H.W. Kim, T.H. Han, Room-Temperature, Highly Durable Ti₃C₂Tx MXene/Graphene Hybrid Fibers for NH₃ Gas Sensing, *ACS Appl. Mater. Interfaces*. 12 (2020) 10434–10442. <https://doi.org/10.1021/acsami.9b21765>.
- [8] Z.U. Abideen, J.H. Kim, A. Mirzaei, H.W. Kim, S.S. Kim, Sensing behavior to ppm-level gases and synergistic sensing mechanism in metal-functionalized rGO-loaded ZnO nanofibers, *Sensors Actuators, B Chem.* 255 (2018) 1884–1896. <https://doi.org/10.1016/j.snb.2017.08.210>.
- [9] J. Choi, Y.J. Kim, S.Y. Cho, K. Park, H. Kang, S.J. Kim, H.T. Jung, In Situ Formation of Multiple Schottky Barriers in a Ti₃C₂ MXene Film and its Application in Highly Sensitive Gas Sensors, *Adv. Funct. Mater.* 30 (2020) 1–9. <https://doi.org/10.1002/adfm.202003998>.